

Full Length Research Paper

Synthesis and Characterization of Iron Oxide Nanoparticles from Wonderful Kola seed for Future Application in Microwave Tumour Ablation

Morakinyo Aderonke Deborah^{1*}, Ibeh Joseph Godwin¹, Aweda Adebayo Moses², Adeyemi David Kehinde³, Oyenyin Aliyu Ope⁴, Ige Olumide¹, Ibitoye Ayo Zaccheus² and Adeneye Samuel Olaoluwa²

¹Department of Physics, Faculty of Science, Nigerian Defence Academy, Kaduna, Nigeria.

²Department of Radiation Biology, Radiotherapy and Radiodiagnosis, College of Medicine/Lagos University Teaching University, Idi-Araba, Lagos, Nigeria.

³Department of Pharmaceutical Chemistry, College of Medicine, University of Lagos, Idi-Araba, Lagos, Nigeria.

⁴Nigerian Navy Reference Hospital, Navy Town, Ojo Barracks, Lagos, Nigeria.

Received 18 July, 2020; Accepted 24 August, 2020

The green method of synthesizing nanoparticles is an eco-friendly, reliable and cost effective approach which has proven to be an alternative to chemical based methods over the years (Dipankar and Murugan, 2012). This research focuses on the synthesis and characterization of super-paramagnetic iron oxide nanoparticles (FeNPs), adopted a co-precipitation procedure by the interaction of ferric chloride solution (precursor) with aqueous extract of wonderful kola seed. The characterization phase was investigated using the Ultra-violet visible spectroscopy, Fourier Transform Infra- red, X-ray Diffraction and Scanning Electron Microscopy. The SEM analysis showed that the particles have irregular shapes with the average particle diameter measured between 10 to 40 nm. The crystalline nature of the nanoparticles was confirmed by the X-ray diffraction method with the crystallite size range between 10 and 47 nm. The absorbance peak of the synthesized wonderful kola FeNPs was investigated using the ultra-violet visible spectroscopy with wavelengths of 431, 488, 613 and 642 nm and corresponding band gap energies of 2.87, 2.54, 2.02 and 1.93eV respectively; while the absorbance peak of wonderful kola extract has a wavelength of 256 nm with band gap energy of 4.84 eV showing the tendency of a new compound formed. The FTIR peak at 3336.0cm^{-1} corresponds to the $-\text{OH}$ bond stretching, with a strong and broad peak intensity (S, B) indicating the presence of alcohols and phenol. The peak value at 1636.3cm^{-1} corresponds to $\text{C}=\text{O}$ bond stretching vibration with strong intensity, indicating the presence of carbonyl and acids. The peak values also denote the change in fundamental vibrational levels of most molecules present in the sample. The synthesized magnetic nanoparticles could be applied as an enhancement tool in microwave tumour ablation.

Key words: Iron oxide nanoparticle, wonderful kola (*Bulchholzia coriacea*), super-paramagnetic, phytochemicals, FeNP characterization.

INTRODUCTION

Microwaves occupy that portion of the electromagnetic spectrum between frequencies of 300 MHz and 300 GHz.

Microwave ablation technique is similar to radiofrequency ablation in that it uses heats to destroy tissues. In the

microwave frequency range, energy is deposited into tissues through waveguides or antennas (called applicators). Microwave ablation allows for flexible approaches to treatment of tumours through percutaneous, laparoscopic and open surgical access. With either computed tomographic or ultrasound guidance, the tumor is localized and the applicator is inserted. Because of the inherent properties of the electromagnetic wave, the device does not need to be grounded, thus alleviating the problem of grounding pad burns. The commonly used frequency bands for microwave ablation are 915 MHz and 2.45 GHz. Other frequencies explored for therapeutic applications include 433 MHz and broadband pulses with frequencies between 1 GHz and 10 GHz (Brace, 2011). Due to the fact that water molecules (H₂O) are polar; when an oscillatory electric field interacts with water molecules, it causes the molecules to flip. As a result of the radiation interaction, the polar water molecules flip back and forth depending on the frequency of the microwave resulting in temperature increase. Therefore, microwave heats matter by agitating water and other polar molecules in the surrounding tissue, thus inducing cellular death via tissue coagulation and necrosis (Simon et al., 2005) at sufficiently high temperature. The temperature profile in tissue during ablation is obtained by solving a bio-heat equation according to Pennes (1948), for modeling thermal therapy procedures. The bio-heat equation is given by:

$$\rho c \frac{dT}{dt} = \nabla(k\nabla T) + Q_s + Q_p + Q_m \quad (1)$$

Where ρ [kg/m³] is the tissue density, c [J/kg⁻¹] is the specific heat of the tissue, k [W/m⁻¹] is thermal conductivity, T [K] is the temperature, Q_s [W/m³] is the absorbed energy, Q_p [W/m³] is the heat loss due to microvascular blood perfusion and Q_m [W/m³] is the metabolic heat generation. The survival fraction of cells in tissue exposed to elevated temperature is given by:

$$\Omega(t) = \ln \left[\frac{C(0)}{C(t)} \right] = \int_0^t A \exp \left\{ -\frac{E_a}{RT(\tau)} \right\} dt \quad (2)$$

Where, $C(0)$ is the original concentration of healthy cells prior to heating, $C(t)$ is the concentration of undamaged cells after heating, Ω is a dimensionless cell damage parameter. A (s⁻¹) is frequency factor, E_a (J/mol) is the activation energy required to transform tissue from normal to damaged state, R [J/mol-K] is the universal gas constant and T (K) is the absolute temperature of tissue. Percentage of dead tissue P can be determined using the Equation:

$$P = 1 - e^{-\Omega} \quad (3)$$

From Equation 3, when $\Omega = 1$, there is 63% probability of cell death and when $\Omega = 4.6$, then the probability of cell death rises to 99%. The first case of $\Omega = 1$ corresponds to when tissue coagulation first occurs and tissue perfusion ceases. To improve the efficacy of these treatments, nanoparticles are currently being studied in combination with non-surgical microwave ablation regimens, in addition to better thermal effect on tumor ablation, nanoparticles can deliver anticancer therapeutics that show synergistic anti-tumor effect in the presence of heat (Rachel et al., 2003). Understanding the molecular mechanism of nanoparticle-mediated tumor ablation could further help engineer nanoparticles of appropriate composition and properties to synergize the ablation process. When magnetic nanoparticles are injected into tumours, their magnetic properties are intensified, due to the complex susceptibility χ'' . Consequently, the external H-field applied also plays an important role in the heating process. It is observed that the power dissipation is proportional to the square of the amplitude of the H field intensity. Therefore, in the bio-heat Equation 1, we include an additional term in Qext:

$$P_t C_t \frac{\partial \tau}{\partial t} = k \frac{\partial^2 \tau}{\partial x^2} - \omega_b P_b C_b (T - T_0) + Q_{met} + \frac{1}{2} \sigma_t |E|^2 + \pi \mu_0 \chi'' f |H|^2 \quad (4)$$

With nanoparticles injected into a tumour, the heating effect is produced by both the electric and magnetic fields generated by the applicator. When magnetic nanoparticles are present, the relation between the specific absorption rate (SAR) and the time rate of change of the temperature in the magnetic material is often expressed as;

$$SAR = \frac{cV_s}{m} \frac{dT}{dt} \quad (5)$$

Where c is the specific heat capacity of the sample, m is the mass of the magnetic particles, V_s is the total volume of the tissue containing the nanoparticle and dT/dt is the temperature increase.

The specific absorption rate SAR is also proportional to the volumetric power dissipation P and can be written as:

$$SAR = \rho * P = \rho \pi \mu_0 \chi'' f |H|^2 \quad (6)$$

Where, ρ represents the density of nanoparticle.

The potential benefits of microwave technology include consistently higher intra-tumoral temperatures, larger

*Corresponding author. E-mail: physic29@gmail.com.



Figure 1. The processing and extraction phase of aqueous wonderful kola (a) Shredded and dried wonderful kola seeds; (b) Pulverization of shredded seeds using a blender (Binatone brand); (c) Dispersion and preparation of powdered wonderful kola seed in distilled water to facilitate extraction.

tumor ablation volumes, shorter ablation times, ability to use multiple applicators, improved convection profile, optimal heating of cystic masses and less procedural pain (Prakash, 2010). Biosynthesis, characterization and application of plant mediated metallic nanoparticles could reduce the exposure of patient to high dose of ionizing radiation. Microwave ablation has been reported to overcome most challenges associated with radiofrequency ablation (Ibitoye et al., 2016), hence the interest for this research work. The dynamic and unlimited applications of magnetic iron oxide nano-sized particles vary from industrial, medical, engineering to general applications. With a focus on the medical application of magnetic nanoparticles, its application varies from biosensors, magnetic resonance imaging, diagnostics, tissue engineering, theranostics, hyperthermia, magnetic separation to drug targeting and delivery (CD Creative Diagnostics and bio-particles products, 2009-2020). Numerous physical and chemical approaches have been formulated for the synthesis of nanoparticles of desired shape, wavelength, absorbance and size. Therefore, green synthesis has been considered as one of the promising methods for synthesis of nanoparticles because of their bio-compatibility, low toxicity and eco-friendliness in nature (Malik et al., 2014). The phytochemicals present in aqueous wonderful kola seeds function as a highly potent reducing and stabilizing agents for metals and as capping agents to create a sustainable coating on the metallic NP nanoparticles in a single step ([https://uses.plantnetproject.org/en/Buchholzia_thollaniana_\(PROTA\)#other_botanical_information](https://uses.plantnetproject.org/en/Buchholzia_thollaniana_(PROTA)#other_botanical_information)).

MATERIALS AND METHODS

Purchase of experimental materials and identification

The seeds of the wonderful kola plant (*Buchholzia coriacea*) were

purchased from the central market of Kaduna Metropolis and Oshodi market in Lagos State. The seeds were identified and validated at The University of Lagos Herbarium, Department of Botany, Akoka, Lagos with identification credentials of the seeds stated as (Scientific name: *B. coriacea*, family: *Capparaceae*, LUH: 8248, Determinavit: Mr Nodza). The purity of ferric chloride hexahydrate, deionized water and other solvents used were strictly kept in check and ascertained to be of standard quality.

Processing and extraction of wonderful kola seeds

Ten wonderful kola seeds were washed meticulously with distilled water to remove dirt, epiphytes and decaying residues. The seeds were shredded and shade dried at ambient temperature for a period of 3 weeks. An electric food processor blender (Binatone brand) was used to pulverize the dried seeds. 20 grams of powdered wonderful kola seed was dissolved in 200 ml of distilled water in a beaker and mixed homogeneously. The mixture was covered with an Aluminum foil, placed inside a water bath, covered and boiled at 60°C for 1 h to facilitate extraction. After boiling for an hour, the broth content was sieved into a clean beaker using a filter and Whitman filter paper to extract the filtrate and stored at 4° C for experimental use in accordance to the research study of Adelere et al. (2017). Figures 1 to 3 show the extraction phase of wonderful kola.

Synthesis of wonderful kola FeNPs

The aqueous extract of wonderful kola was used to synthesize iron nanoparticles where 0.2M of FeCl_3 was reacted with 30 g/l of wonderful kola extract in a ratio of 2:3 at room temperature with constant stirring. An instant colour change from transparent pink to mild brown colour was observed. Furthermore, while stirring the mixture, 1.0 M of NaOH solution (prepared in 100 ml) was added to the mixture dropwise until a pH of 6.0 was achieved in accordance to Shahwan et al. (2011). A gradual colour change from mild brown to rusty brown colour was obtained. The introduction of the chloride of ferric solution to serve as a precursor agent to the wonderful kola seed extract (containing tannin, flavonoid, glycoside, saponins and alkaloids) possibly resulted in the reduction of iron salt component and nanoparticle stabilization. The activity of the hydroxyl group (OH) in the reduction of iron salt brought about a decline in the pH of the sample during the synthesis of iron oxide NPs. In the chemical reaction, the hydrolyzation of iron chloride (FeCl_3) solution



Figures 2. Synthesized FeNPs in Wonderful kola extract (a) After synthesis, the color of the wonderful kola extract solutions at ambient temperature rapidly changed from clear pink to rusty brown, signaling the likely formation of FeNPs. (b) Synthesized WK FeNP.

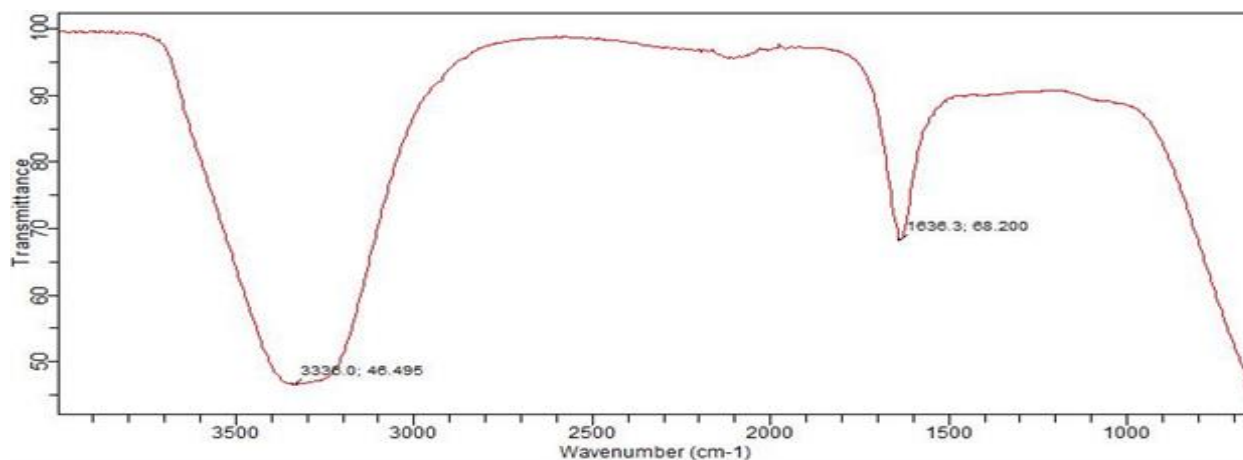


Figure 3. Fourier Transform Infra-red spectrum for Synthesized Wonderful kola seed FeNPs. Sample ID: WONDERFUL KOLA FeNP, Method Name: Transmittance Method, Sample Scans:30, Resolution:8, Range: 4000 – 650 wave number (cm^{-1}).

resulted in the formation of ferric hydroxide, which later releases H^+ ions. The aqueous wonderful kola seed extract (R) in the reaction partially reduces the ferric hydroxide to form FeNPs with the oxidation of the aldehyde group to respective acids in relation to the study of Mahdavi et al. (2013) and Becerra et al. (2007). The presence of other organic compounds contained in the wonderful kola seed extract also aided the synthesis process to stabilize the value of the pH at 6, a prerequisite for enzymic reactions (Kanagasubbulakshmi and Kadirvelu, 2017). The biological reduction of iron oxide by the aqueous extract of wonderful kola seed for the synthesis of FeNP nano-sized particles was followed by centrifugation procedure for the isolation of Iron oxide NP from other compounds present in the sample. The prepared sample was transferred to new sample bottles and centrifuged at 1200rpm for 20 min. The surfactant was extracted from the supernatant into fresh sample bottles for drying at ambient temperature and also for characterization purpose.

Characterization of wonderful kola FeNPs

Different phases of characterization to ascertain the physical,

chemical and morphological parameters of the synthesized wonderful kola seed nanoparticles were carried out which include: Fourier Transform Infra-red Spectroscopy (FTIR model, Cary 630, Agilent technologies, USA), X-Ray Diffraction (XRD model, EMPYREAN by Malvern Panalytical UK.), Ultraviolet Visible Spectroscopy (UV-Vis model, T90+ UV/VIS Spectrometer, PG Instruments Limited), Scanning Electron Microscopy (SEM model, Phenom ProX, by PHENOMWORLD ENDHOVEN the Netherlands).

RESULTS AND DISCUSSION

Fourier transform infra-red spectroscopy

Fourier transform (a mathematical process) was adopted to transform the raw information into the infrared spectrum (Griffith et al., 2007) in this research study. FTIR Spectroscopy was adopted as a tool to identify the functional groups of the key elements with regards to determining the peak point (Full Width, Half Maximum FWHM) in the spectrum. Figure 3 depicts the FTIR

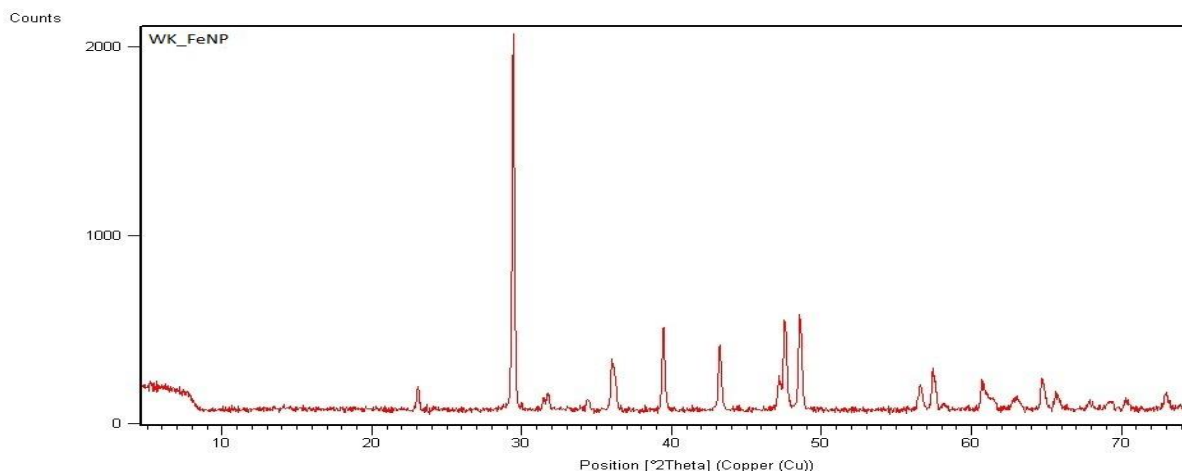


Figure 4. The X-ray Diffraction Pattern of Synthesized wonderful kola FeNPs.

spectrum of synthesized wonderful kola FeNPs obtained.

The FTIR analysis shows the stretching vibrations at 3336.0 and 1636.3 cm^{-1} with corresponding transmittance at a value of 46.495 and 68.200 , respectively (Figure 3); it falls in the mid-infrared IR spectrum region of 400 to 4000 cm^{-1} . The interpretation of the FTIR peak at 3336.0 cm^{-1} corresponds to the $-\text{OH}$ bond stretch, with a strong and broad peak intensity (S, B). It indicates the presence of alcohols and phenols denoting the aqueous phase as well as aiding the reduction of the ferric chloride. The peak value at 1636.3 cm^{-1} corresponds to $\text{C}=\text{O}$ bond stretch with strong intensity, indicating the presence of carbonyl and acids. This indicates the metabolites and phytochemicals available in the wonderful kola extract and amino acids, which aids the capping and stabilization process in the formation of FeNPs (<https://www.compoundchem.com/>). The peak values also depict the change in fundamental vibrational levels of most molecules present in the sample. The presence of traces of organic acid is denoted by unlabeled and visible peaks. These peaks reduce the pH of the samples which aids the synthesis of wonderful kola FeNPs (www.masterorganicchemistry.com).

X-Ray diffraction

The crystallinity in terms of the structure and the phase identification of the wonderful kola nano-sized particle was determined and analyzed by x-ray diffraction technique. Figure 4 depicts the x-ray diffraction of synthesized wonderful kola FeNPs. The presence of diffraction peaks with 2θ values of 23.0° , 29.4° , 31.6° , 34.4° , 36.0° , 39.4° , 43.2° , 47.5° , 48.5° , 56.6° , 57.4° , 60.6° , 64.6° corresponds to d_{spacing} value of 0.39 , 0.30 , 0.28 , 0.26 , 0.25 , 0.23 , 0.21 , 0.19 , and 0.14 nm respectively of wonderful kola nano-sized crystals as

obtained from Figure 4. The data obtained were compared with literatures and are in agreement with the x-ray diffraction standard for superparamagnetic nanoparticles (Table 1). The Debye Scherrer equation was adopted to calculate the average crystallite particle sizes which ranges approximately from 10 to 47 nm . The Debye Scherrer equation defines the relationship between the peak broadening and particle size in X-ray diffraction as denoted by the equation below (Patterson, 1939):

$$d = \frac{k\lambda}{(\beta \cdot \cos\theta)} \quad (7)$$

Equation 7: The Debye Scherrer Equation. Particle size of the crystal (nm) is d , Scherrer constant is k (dimensionless) (ranges from 0.9 to 1.0), x-ray wavelength is λ (0.15406 nm), width of the XRD peak at half-maximum is β (radian), bragg's diffraction angle is θ (degrees). The value of the inter plane spacing

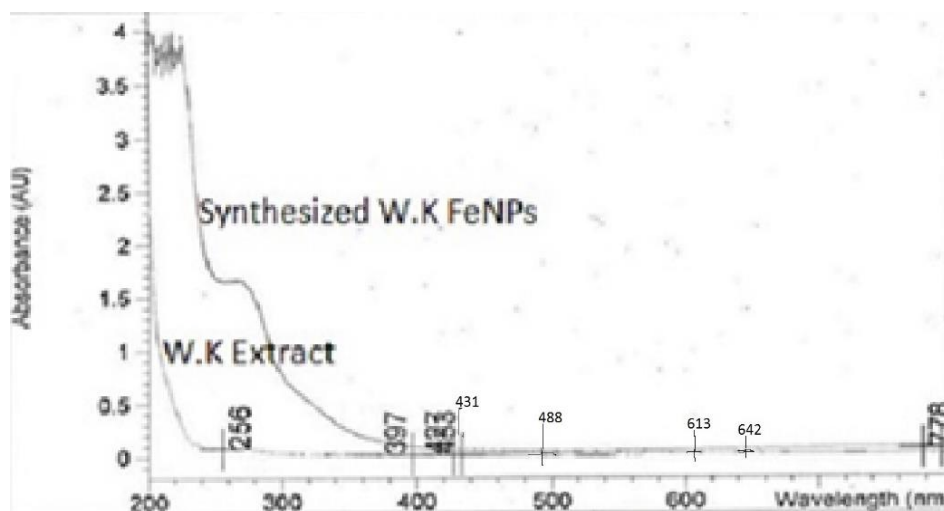
Ultra-violent visible spectroscopy

The Ultraviolet-visible spectroscopy is termed as the absorption spectroscopy in the UV-Visible spectral region. It makes use of light in the visible and adjacent (near – UV and near-infrared) ranges. In this region of the electromagnetic spectrum, molecules undergo electronic transitions (Skoog et al., 2007) (Figure 5).

In this research study, the absorbance peak of wonderful kola extract has a wavelength of 256 nm absorbance 1.65340 AU with band gap energy of 4.84 eV . The absorbance peak of synthesized wonderful kola FeNPs displayed an onset of broad absorption maxima at wavelength of 431 nm (absorbance 0.10047 AU), 488 nm (absorbance 0.15959 AU), 613 nm (absorbance 3.7274 E-3)

Table 1. Variation of inter plane spacing (d_{hkl}), 2θ , θ , full width half maximum (FWHM) and crystallite particle sizes.

S/N	d_{hkl} / Inter plane Spacing (nm)	2 Theta (°)	Theta (°)	FWHM (λ)	Crystallite particle size (nm)
1	0.39	23.036	11.518	0.364	23.26
2	0.30	29.406	14.703	0.182	47.12
3	0.28	31.408	15.704	0.728	11.84
4	0.26	33.462	16.731	0.280	31.01
5	0.25	35.984	17.992	0.442	19.74
6	0.23	39.416	19.708	0.234	37.65
7	0.21	43.186	21.593	0.332	26.87
8	0.19	47.528	23.764	0.286	31.69
9	0.19	48.516	24.258	0.312	29.17
10	0.16	56.524	28.262	0.572	16.47
11	0.16	57.382	28.691	0.380	24.89
12	0.15	60.632	30.316	0.988	9.73
13	0.14	64.662	32.331	0.546	17.98

**Figure 5.** Comparison of the UV-Vis spectrum of aqueous wonderful kola with synthesized FeNPs.

and 642nm (absorbance 7.5321×10^{-2}), accordingly in visible range between 200 to 800 nm wavelength. This indicates the formation of FeNPs having rusty brown color, which was investigated using the Ultra-violet visible spectroscopy. Band gap energy is calculated with respect to the Equation

$$E_{bg} = \frac{1240}{\lambda} (eV) \quad (8)$$

E_{bg} is the band-gap energy and λ is the wavelength of the nanoparticle. Corresponding band gap energies with reference to the wavelengths are 2.87, 2.54, 2.02 and 1.93eV. The presence of more than one broad absorption peaks at different wavelengths indicates the formation of

iron nanoparticles which is believed to be due to the residue of collective oscillation of surface plasmons, with exposure to air new absorption bands appear as a result of oxidation with several maxima depicting the presence of numerous iron oxide nanoparticles in relation to the study of Klacanova et al. (2012).

Scanning electron microscopy

The Scanning Electron Micrograph (SEM) and Image-J software were adopted in this research to study the size distribution and measurement parameters of wonderful kola FeNPs. The average size of the Wonderful kola FeNPs was in the range of 10 to 40 nm. The nanoparticles in Figures 6 to 8 were observed to have inhomogeneous

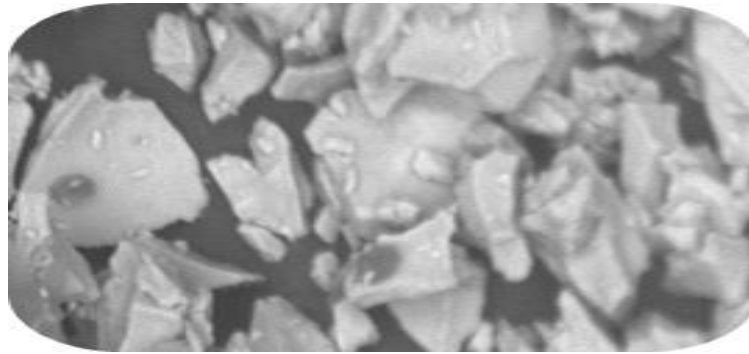


Figure 6. SEM Image of wonderful kola FeNPs.Magnification 1000x, 15Kv-image BSD Full.

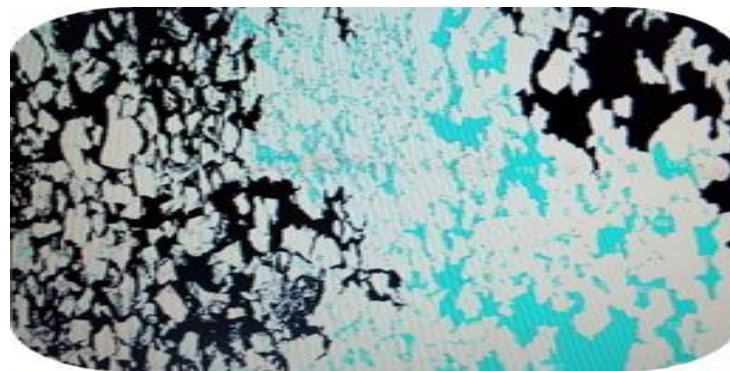


Figure 7. Image j processed SEM result. Magnification 1018x1014, 8-bit (Inverting LUT);1008k.

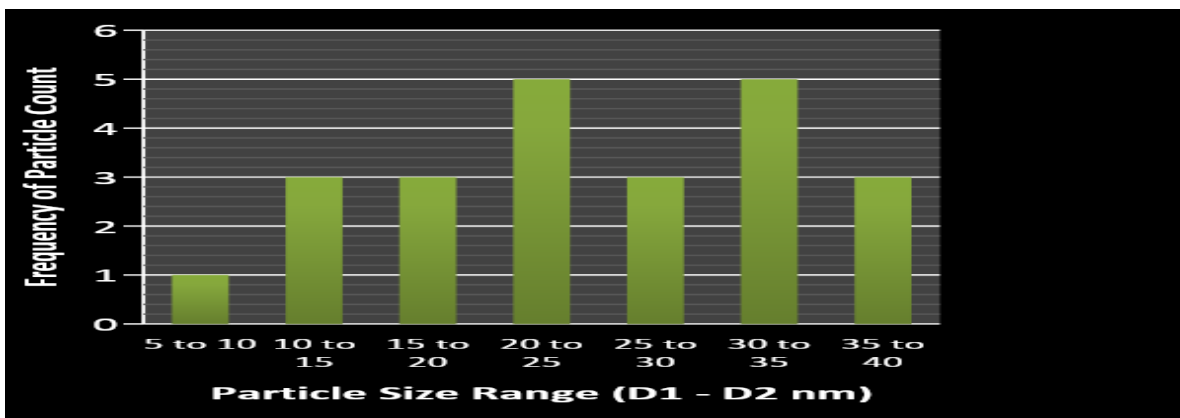


Figure 8. The graphical representation of the particle size range (nm).

and irregular shapes (octahedral, spherical and unquantifiable shapes as shown above). The physical and structural features of the synthesized nano-sized particle are largely affected by the irregular shape of the NP induced by the constituent of the synthesized sample (Table 2).

Conclusion

The use of wonderful kola seed in the synthesis of zero-valent super-paramagnetic nano-sized particles was achieved. The co-precipitation method adopted proved effective and easily replicated. A colour change from clear

Table 2. The particle size range (nm) and the frequency of particle count.

S/N	Particle size range (s)	Frequency of particle count
1	5 - 10	1
2	10 - 15	3
3	15 - 20	3
4	20 - 25	5
5	25 - 30	3
6	30 - 35	5
7	35 - 40	3
8	40 - 45	-
9	45 - 50	-
10	50 - 100	-
11	> 100	-

pink to rusty brown was observed from the synthesis of wonderful kola iron oxide nanoparticle. In the XRD peak analysis, the Debye Scherer equation was adopted to calculate the crystallite particle sizes which ranges approximately from 10 to 47 nm. The crystallite particle sizes as depicted by the SEM analysis ranges from 10 to 40 nm, with the presence of irregular shapes (octahedral, spherical, cubic and other unspecified shapes). The FTIR peak at 3336.0 cm^{-1} corresponds to the $-\text{OH}$ bond stretch, with a strong and broad peak intensity (S, B) indicating the presence of alcohols and phenols denoting the aqueous phase as well as aiding the reduction of the ferric chloride. The peak value also shows traces of N-H stretch with a medium intensity, indicating the presence of amine and amides. The peak value at 1636.3 cm^{-1} corresponds to C=O bond stretch with strong (S) intensity, indicating the presence of carbonyl and acids. This denotes the phytochemicals available in the wonderful kola extract and amino acids, which aids the capping and stabilization process in the formation of FeNPs. The peak values also depict the change in fundamental vibrational levels of most molecules present in the sample. In the UV-Vis spectrum analysis, the absorbance peak of wonderful kola extract has a wavelength of 265 nm with band gap energy of 4.68 eV. The absorbance peak of synthesized WK FeNPs has a wavelength of 431, 488, 613 and 642 nm accordingly which was investigated using the ultra-violet visible spectroscopy; corresponding band gap energies with reference to the wavelengths are 2.87, 2.54, 2.02 and 1.93 eV.

ACKNOWLEDGEMENT

The authors are grateful to the Nigerian Defence Academy, Department of Physics, Kaduna, The College of Medicine, Department of Radiation Biology, Radiotherapy and Radio diagnostics, Department of

Pharmaceutical Chemistry, Central Research Laboratory (The College of Medicine, University of Lagos, Nigeria). This research study was supported by the Nigerian Defence Academy, Ribadu Campus, Kaduna State, Nigeria.

CONFLICT OF INTEREST

The authors declare no conflict of interest.

REFERENCES

- Adelere IA, Agbaje L, Aboyeji DO, Abdulsalam R, Adabara NU, Bala JD (2017). Biosynthesis of Silver Nanoparticles Using Aqueous Extract of *Buchholzia Coriacea* (Wonderful kola) Seeds and Their Antimicrobial Activities. *Annals Food Science and Technology* 18(4):1-4.
- Becerra RH, Zorrilla C, Ascencio JA (2007). Production of iron oxide nanoparticles by a biosynthesis method: An environmentally friendly route. *Journal of Physical Chemistry* 111(44):16147-16153.
- Brace CL (2011). Microwave Tissue Ablation biophysics, Technology and Applications. *Critical Reviews in Biomedical Engineering* 38(1):65-78.
- CD Creative Diagnostics and bio-particles products, (2009 - 2020) Properties and applications off magnetic nanoparticles. (https://www.cd-bioparticles.com/t/properties-and-applications-of-magnetic-nanoparticles_55.html)
- Dipankar C, Murugan S (2012). The green synthesis, characterization and evaluation of the biological activities of silver nanoparticles synthesized from *iresine herbstii* leaf aqueous extract, *Colloids and Surfaces, Sciencedirect: Bio interface* 98:112-119.
- Griffith PR, De Hasseth JA, Winefordner JD (2007). *Fourier Transform Spectroscopy*, 2nd Edition, Wiley-Blackwell. pp. 1-560. [https://uses.plantnetproject.org/en/Buchholzia_thollaniana_\(PROTA\)#ot-her_botanical_information](https://uses.plantnetproject.org/en/Buchholzia_thollaniana_(PROTA)#ot-her_botanical_information)
- Ibitoye AZ, Nwoye EO, Aweda AM, Oremosu AA, Anunobi CC, Akanmu NO (2016). Microwave ablation of *ex vivo* bovine tissues using a dual slot antenna with a floating metallic sleeve. *International Journal of Hyperthermia* 32(8):923-930.
- Kanagasubbulakshmi S, Kadirvelu K (2017). Green Synthesis of Iron Oxide Nanoparticle using *Lagenaria Siceria* and Evaluation of its Antimicrobial Activity. *Defence Life Science Journal* 2(4):422-425.
- Klaczanova K, Fodran P, Simon P, Rapta P, Boca R, Jori V, Miglierini M, Kolek E, Caplovic L (2012). Formation of Fe(O) – Nanoparticles via

- reduction of Fe (II) compounds by amino acids and their subsequent oxidation to iron oxides. Hindawi Publishing Corporation. Journal of Chemistry 2013:1-10.
- Mahdavi M, Farideh N, Mansor BA, Rosfarizan M (2013). Green biosynthesis and characterization of magnetic iron oxide (Fe_3O_4) nanoparticles using seaweed (*Sargassum muticum*) aqueous extract. Molecules 18(5):5954-5964.
- Malik P, Shankar R, Malik V, Sharma N, Mukherjee TK (2014). Green chemistry based benign routes for nanoparticle synthesis. Journal of Nanoparticles 2014:1-14.
- MasterOrganicChemistry
https://www.google.com/amp/s/www.masterorganicchemistry.com/2016/11/23/quick_analysis_of_ir_spectra/amp/ Accessed March 10th, 2020.
- Patterson A (1939). The Scherrer formula for x-ray particle size determination. American Physical Society 56(10):978-982.
- Pennes HH (1948). Analysis of Tissue and Arterial Blood Temperatures in the Resting Human Forearm. Journal of Applied Physiology 1(1):93-122.
- Prakash P (2010). Theoretical modeling for hepatic microwave ablation. The Open Biomedical Engineering Journal 4:27-38.
- Rachel L, Kashif A, Minh L, Nancy LO (2003). Fluorescence Resonance energy transfer reveals a binding site of a photosensitizer for photodynamic therapy. Cancer Research 63(17):5194-5197.
- Shahwan T, Abu SS, Nairat M, Scott TB (2011). Green synthesis of iron nanoparticles and their applications as a fenton-like catalyst for the degradation of aqueous cationic and anionic dyes. Elsevier, Chemical Engineering Journal 172(1):258-266.
- Simon CJ, Dupuy DE, Mayo-Smith WW (2005). Microwave ablation: principles and applications. RadioGraphics 25:S69-S83.
- Skoog DA, Holler FJ, Crouch SR (2007). Principles of Instrumental Analysis, 6th edition, Belmont, CA. Thomson books/cole pp.169-173.